J Mol Model (2006) 12: 205–212
DOI 10.1007/s00894-005-0019-5

ORIGINAL PAPER

Tomasz Grabarkiewicz · Marcin Hoffmann

Syn- and *anti*-conformations of 5′-deoxy- and 5′-O-methyl-uridine 2′,3′-cyclic monophosphate

Received: 31 January 2005 / Accepted: 22 June 2005 / Published online: 18 August 2005

Abstract Two uridine 2′,3′-cyclic monophosphate (cUMP) derivatives, 5′-deoxy (DcUMP) and 5′-O-methyl (McUMP), were studied by means of quantum chemical methods. Aqueous solvent effects were estimated based on the isodensity-surface polarized-continuum model (IPCM). Gas phase calculations revealed only slight energy differences between the *syn*- and *anti*-conformers of both compounds: the relative energies of the *syn*-structure are −0.9 and 0.2 kcal mol^{-1} for DcUMP and McUMP, respectively. According to the results from the IPCM calculations, however, both *syn*-conformers become about 14 kcal mol^{-1} more stable in aqueous solution than their corresponding *anti*-structures. Additionally, the effects of a countercation and protonation on DcUMP were studied, revealing that the *syn*-structure is also favored over the *anti*-one for these systems.

Keywords cUMP · *syn-anti*-conformations · C-H···O hydrogen bond · DFT method

Introduction

The analysis of structural properties of nucleic-acid constituents is of great importance for understanding their biological function. Even more exciting, for any biomolecular system, is the analysis of the relationship between structure and energy. So far, many experimental measurements and theoretical analyses have been undertaken to study the molecular structure of elementary building blocks of nucleic acids. [1,2,3,4] Although X-ray or NMR experiments provide the most valuable information about the structure of nucleic acids, they are unable to reveal the energy differences between their various forms. The application of modern computational methods can overcome this limitation, serving as a convenient way to unravel the essential links between conformational and energetic properties.

It is generally accepted that hydrogen bonding plays a key role in biomolecular structure and function. [5] This is certainly the most important type of interaction observed in DNA and RNA. [6] From a large set of hydrogen bonds, C-H···O hydrogen bonding deserves particular attention. Although it is less common and usually weaker than others, its importance in the context of biomolecules should not be underestimated. As has been shown, [7, 8] this type of bonding may be a dominant structural feature, in many biomolecules in general, and in nucleotides in particular.

So far, much attention has been given to the conformational behavior of deoxyribonucleosides and ribonucleosides in their most typical conformations. There are many examples of spectroscopic and crystallographic studies concerning this topic. [9,10] They have also been thoroughly studied using empirical, as well as non-empirical calculations. [11,12] Unlike the above-mentioned deoxyribonucleosides and ribonucleosides, their cyclic analogues have not been studied in as much detail, even though the biological role of these molecules is very important. According to the position of oxygen atoms, we can distinguish two major types of cyclic nucleotides: 3′,5′ and 2′,3′ (see Fig. 1). Molecules of the first type are involved in a series of regulatory and hormonal cellular mechanisms, while the second ones were established as a kinetically competent intermediates in the mechanism of Rnase A catalyzed hydrolysis of RNA. Contrary to rather rigid 3′,5′-cyclic nucleotides, the 2′,3′-cyclic ones are characterized by an extraordinary conformational flexibility, which is suspected to be functionally important for the specific behavior of Rnase A. Certainly, the orientation of a nucleobase around the

T. Grabarkiewicz (✉) · M. Hoffmann
Quantum Chemistry Group, Faculty of Chemistry,
A. Mickiewicz University, ul. Grunwaldzka 6,
60-780 Poznan, Poland
E-mail: grabar@man.poznan.pl
Tel.: +48-61-8291289
Fax: +48-61-8658008

M. Hoffmann
BioInfoBank Institute, ul. Limanowskiego 24A,
60-744 Poznan, Poland

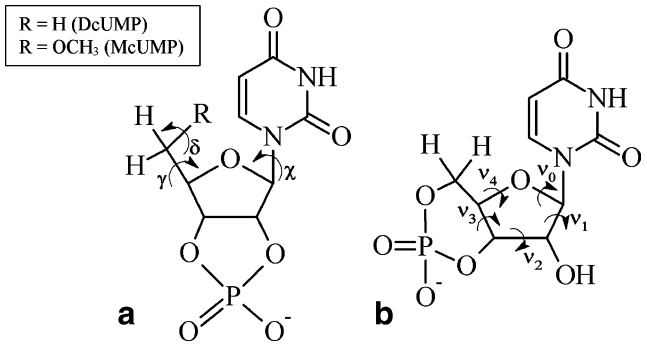

Fig. 1 Chemical formulas of cyclic nucleotides in their ionic forms: uridine 2′,3′-cyclic monophosphate **(a)** and uridine 3′,5′-cyclic monophosphate **(b)**. The major conformational angles of ribonucleotides are shown

glycosidic bond is an essential factor, since an *anti*-orientated nucleobase is responsible for the proper recognition in the active center of the enzyme. [13] It has long been suggested that the *anti*-orientation is favored because of steric hindrance between the base and sugar in the *syn*-orientation. Quite surprisingly, early X-ray and NMR experiments showed that, in the case of 2′,3′-cyclic nucleotides, the situation may look different. [14] The results suggested the preference of the *syn*-orientation over the *anti*-one. A possible connection between these two facts, however, still remains unknown. In order to explain this, a more complete structural study of 2′,3′-cyclic nucleotides is required.

To our knowledge, there is no such study using theoretical methods. Therefore, in this paper, we have undertaken a computational investigation of the structure and energetics of two modified uridine 2′,3′-cyclic monophosphate (see Fig. 1a) derivatives: DcUMP and McUMP. The material presented is part of a more complex study devoted to a series of modified cUMPs to be reported in a forthcoming publication.

Computational methods

All quantum-chemical calculations presented in this paper were performed with the Gaussian03 code [15] at the DFT level of theory, using the hybrid functional B3LYP. [16,17] In the course of final geometry optimization and normal-mode calculations, the split-valence basis sets of 6–31G [18] and 6–311G, [19] augmented with diffuse and polarization functions were used. It is generally accepted that the inclusion of at least one set of diffuse functions is necessary for a proper description of hydrogen-bonded, anionic systems. [20,21] Population analyses using the Mulliken, [22] CHELPG (charges from electrostatic potentials using a grid-based method), [23] and NPA (natural population analysis) [24] schemes were carried out.

The solvent effect was estimated based on a static isodensity-surface polarized-continuum model (IPCM). [25] The choice of method was based on initial trials, using the Onsager model, which, in our opinion, led to significantly underestimated values of solvation energy (especially for the molecular anion). The geometries optimized in the gas phase were taken for single point energy calculations in solution. In such an approach, solvent molecules are not explicitly taken into account. Rather, they are only the source of a continuum field determined by the dielectric constant. Nevertheless, such an approximation proved to provide a valuable insight into the solvation effects.

The pseudorotation phase angle $\boldsymbol{P}$ (0°–360°) and the maximum puckering amplitude $\nu_{\max}$ were calculated according to Altona et al. [26] The endocyclic torsional angles ν_0-ν_4 were defined as in Fig. 1b. Conformations of ribose moieties (see Table 1) were characterized using the E and T notation as shown in Fig. 2.

In order to find the global energy minima of both compounds, potential energy surfaces were calculated at the B3LYP/6–31G(d) level of theory. The torsional angles χ (O4′-C1′-N1-C2) and γ (C3′-C4′-C5′-O5′) were varied from 0° to 360°, in 15-degree increments. The final geometries were located by full energy optimizations, starting from the lowest energy conformations obtained during this discrete sampling. In addition, the zero-point vibrational energy (ZPE) was added to check whether it changes the energy order. The initial ribose conformation was C3′-*endo*—typical for the A form of RNA. Two alternative puckering modes of a five-

Table 1 Selected geometrical parameters of DcUMP and McUMP in various minimum energy conformations

Model Compound	Conformation	χ	γ	δ	P / ribose	$\nu_{\max}$
DcUMP	*syn*/*endo*	**64.8**	–	–	**96.4/** ^{0}E	**35.5**
	syn/*exo*	**66.7**	–	–	**53.7/** $_{4}E$	**29.5**
	anti/*endo*	**−118.2**	–	–	**84.9/** ^{0}E	**40.0**
	anti/*exo*	**−112.2**	–	–	**69.4/** $_{4}E$	**39.1**
McUMP	*syn*/*endo*	**65.1**	**80.2**	**47.0**	**96.0/** ^{0}E	**38.6**
	syn/*exo*	**66.8**	**78.4**	**47.2**	**70.3/** ^{4}E	**36.6**
	anti/*endo*	**−142.2**	**−179.1**	**53.3**	**22.9/** ^{3}E	**30.1**
	anti/*exo*	UNSTABLE				

χ(O4′-C1′-N1-C2),γ(C3′-C4′-C5′-O5′),
δ(C4′-C5′-O5′-C6′),
in degrees; $\boldsymbol{P}$—pseudorotation phase angle,
in degrees; **ribose**—conformation of the ribose moiety (see also Figure 2)

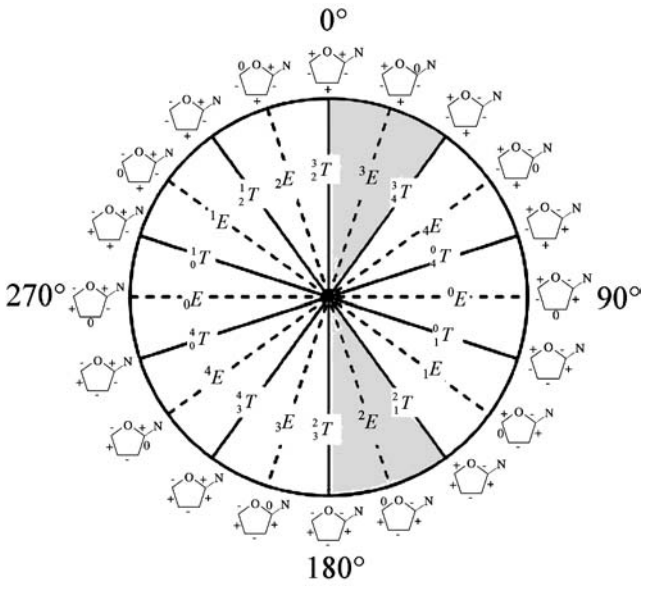

Fig. 2 Pseudorotation wheel of the ribose ring. Each point on the circle represents a specific value of the pseudorotation angle ***P***. Shaded regions indicate most typical conformations found in A- and B-type helices. ^{2}E and ^{3}E correspond to C2′-*endo* and C3′-*endo*, respectively

membered phosphodiester ring were assumed. According to the position of the phosphorus atom in respect of the sugar ring, *endo*- and *exo*-forms were distinguished (see Fig. 3).

Results and discussion

Molecular anion *in vacuo*

As mentioned above, 2′,3′-cyclic nucleotides belong to a structurally flexible group of biomolecules. Because of their many degrees of freedom, a wide range of geometries and more than one minimum-energy conformation are allowed. Therefore, the energies and selected geometrical parameters of only four main conformers (see Figs. 4 and 5) are shown in Tables 1 and 2, respectively. As can be seen, for the isolated systems, all *endo*- forms are more stable than the *exo*-ones. For DcUMP, the global minimum, the *syn*/*endo*-form is 0.9 kcal mol^{-1} lower in energy than the corresponding *anti*/*endo*-form and approximately 1 and 3 kcal mol^{-1} lower than *syn*/*exo* and *anti*/*exo*, respectively. For McUMP, the most stable form is *anti*/*endo*, but the *syn*/*endo*-conformer is only 0.2 kcal mol^{-1} higher in energy. The *anti*/*exo*-conformation seems to be energetically disfavored, since during optimization it undergoes a spontaneous transition to the aforementioned *anti*/*endo*-conformation (see Fig. 3).

Even though the relative energy differences between *syn*- and *anti*-structures are very small for the *endo*-type conformers, it is noteworthy that they correspond to well-defined minima and the energetic barrier of conversion between them would be as high as 6.5 and 7.3 kcal mol^{-1} for DcUMP and McUMP, respectively. This estimation is based on the results of the initial calculations of energy as a function of dihedral angle χ (data not shown). The resultant energy profiles allowed us to evaluate the magnitude of the intrinsic torsional energy barrier between *syn*- and *anti*-conformers at the above level.

It is well known that environmental effects play an important role in the conformational flexibility of nucleotides. The presence of water and metal ions is widely known to affect the energetics of the phosphodiester moiety. The electrostatic repulsion between phosphate groups is reduced because of the high dielectric constant of water and the influence of hydrated counterions. [6]

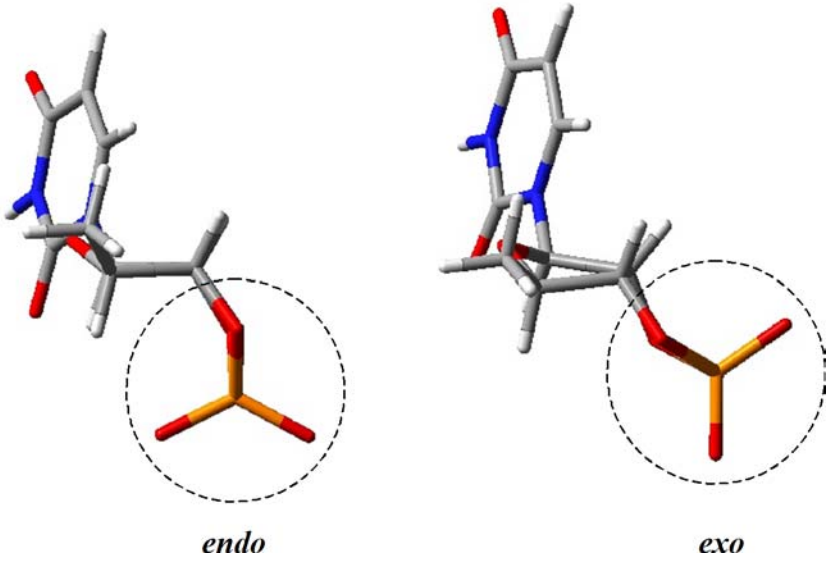

Fig. 3 Possible conformations of the cyclic phosphate ring as observed in DcUMP. The *endo* form is stabilized by the interactions between O2P and H1′ and H2′. The *exo* form is more prone to interact with the aqueous environment (vide infra)

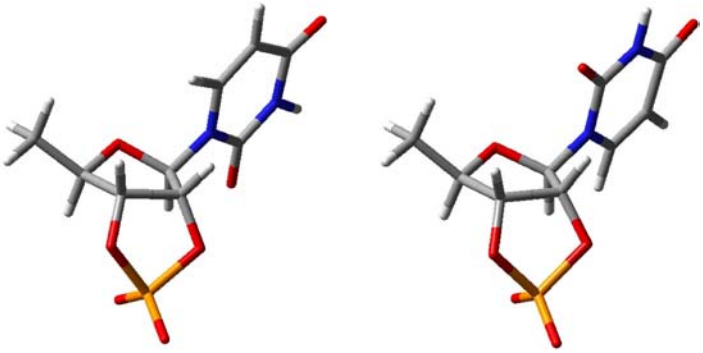

Fig. 4 Gas phase optimized structures of *anti* (left) and *syn* (right) DcUMP. Both structures are in *endo* form

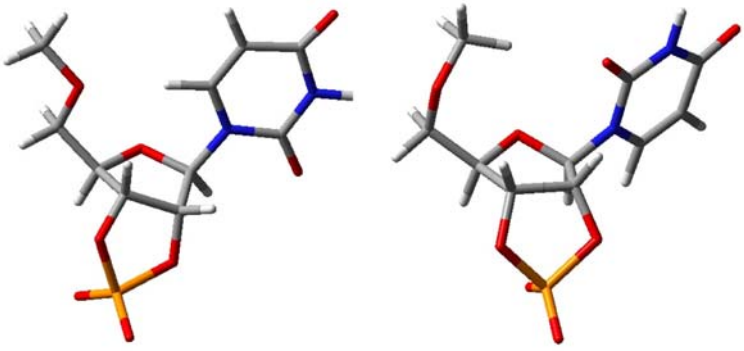

Fig. 5 Gas phase optimized structures of *anti* (left) and *syn* (right) McUMP. Both structures are in *endo* form

Table 2 Relative energy values (kcal mol^{-1}) and dipole moments (debye) of DcUMP and McUMP in various minimum energy conformations obtained at the DFT level of theory

Model Compound	Conformation	Dipole Moment	ΔE_{gas}	ΔE_{aq}	
				IPCM	**Onsager**
DcUMP	*syn*/*endo*	**9.53**	**0.0**[a]	**8.3**	**2.6**
	syn/*exo*	**12.59**	**3.0**	**0.0**[b]	**0.6**
	anti/*endo*	**11.45**	**0.9**	**13.5**	**0.6**
	anti/*exo*	**11.97**	**1.1**	**14.2**	**0.0**[c]
McUMP	*syn*/*endo*	**10.67**	**0.2**	**11.5**	**4.0**
	syn/*exo*	**13.78**	**4.6**	**0.0**[e]	**0.0**[f]
	anti/*endo*	**13.24**	**0.0**[d]	**13.6**	**3.9**
	anti/*exo*	UNSTABLE			

calculated at B3LYP/6-31 + + G(d,p)[a]absolute energy of –1326.65882927 hartree;[b]absolute energy of –1326.78812974 hartree;[c]absolute energy of –1326.67317483 hartree;[d]absolute energy of –1441.17890700 hartree;[e]absolute energy of –1441.29493723 hartree;[f]absolute energy of –1441.19536298 hartree

Molecular anion in solution

To characterize the effect of aqueous solvation, the relative energies of the different geometries were studied in the aqueous phase represented by the IPCM reaction-field model. As expected, the relative energies of the different geometries changed upon the inclusion of the aqueous environment. In fact, the energy differences between the various conformers increased upon going to the aqueous phase. Compared to the gas-phase results, a significant stabilization due to solvation was found for the *syn*/*exo*-conformers of both DcUMP and McUMP. The energy differences between *syn*- and *anti*-conformers increased to 14.2 kcal mol^{-1} in the case of DcUMP and 13.6 kcal mol^{-1} in the case of McUMP. The calculated values of the dipole moments (see Table 2) can serve as an explanation of this observation. Since both conformers have the largest dipole moments, the dipole-induced dipole interactions are more attractive, which in turn stabilizes them in the solvent. Moreover, in the case of *exo*-puckered phosphate rings, both oxygen atoms are more exposed to the solvent and therefore more susceptible to hydrogen bonding.

DcUMP with counter cation

In order to gain insight into the role of metal ions around cUMP derivatives, an electrically neutral system (DcUMP) with a sodium cation was selected. Na^+ is certainly the most common counterion observed in nucleic acids. Even though its interactions with the phosphate groups are known to occur through specific complexation with water molecules, [6] the results of some previous calculations [27] validated the choice of Na^+ for a proper description of the long-range electrostatic effects.

The results obtained are shown in Table 3. As shown in Fig. 6, two alternative positions of metal ion were established:

- (**anti I** and **syn**) in the same plane as O1P-P-O2P and similarly distant (2.22 Å) from O1P and O2P
- (**anti II**) in the same plane as O2P-P-O2′ and between O2P and O2 (O2P-Na distance equal to 2.16 Å, Na-O2 distance equal to 2.21 Å and O2P-Na-O2 angle equal to 139.8°)

Even though **anti II** was the lowest-energy structure in the gas phase, it turned out to be significantly less stable when solvent effects were taken into account. A brief examination of some major geometrical parameters ($_1E$ conformation of the sugar ring and $\chi = -151.3°$) reveals a considerable structural distortion of **anti II** as compared to the other *anti*-conformers. This unfavorable geometry might be responsible for its remarkable destabilization in aqueous solution.

In addition, a complete set of Mulliken, NPA, and CHELPG partial atomic charges is presented in Tables 4 and 5. As it is clearly seen and has been noted previously, [28] the atomic charges obtained with different methods vary appreciably. However, we include them for the sake of comparison, since they provide a general view of the tendency of the global charge redistribution after the inclusion of the metal ion into the system.

Protonated neutral form of DcUMP

An alternative way of neutralizing the negative charge of the phosphate group can be achieved simply by protonation of one of the oxygen atoms. At first, the energetic preferences of the protonation sites were tested in the gas phase. As seen from Table 3, there is a negligible difference in energy between the O1P and O2P protonated forms of DcUMP (0.1 kcal mol^{-1} for both con-

Table 3 Relative energy values (kcal mol^{-1}) and dipole moments (debye) of DcUMP in different neutralized forms obtained at the DFT level of theory

Model Compound	Conformation		Dipole Moment	ΔE_{gas}		ΔE_{aq} IPCM	IPCM	Onsager
DcUMP	*syn* Na^+		**9.34**	**7.3**	**4.7**	**0.0**[c]	**0.0**[d]	**1.2**
	anti Na^+	*I*	**8.30**	**8.6**	**5.6**	**20.7**	**5.2**	**3.4**
		II	**6.43**	**0.0**[a]	**0.0**[b]	**32.1**	**23.9**	**0.0**[e]
	syn H^+	*O1P*	**0.78**	**0.0**[f]	**0.0**[g]	**0.0**[h]	**0.0**[i]	**0.0**[j]
		O2P	**3.91**	**0.1**	**0.3**			
	anti H^+	*O1P*	**5.72**	**2.7**	**2.3**	**16.7**	**16.7**	**1.3**
		O2P	**4.82**	**2.6**	**2.2**			

[a,c]calculated at B3LYP/6-31G(d);
[b,d,e]calculated at B3LYP/6-31 + + G(d,p)
[a]absolute energy of –1488.89426397 hartree;
[b]absolute energy of –1488.94983126 hartree;
[c]absolute energy of –1489.01576171 hartree;
[d]absolute energy of –1489.06050865 hartree;
[e]absolute energy of –1488.95458198 hartree;
[f]absolute energy of –1327.10573204 hartree;
[g]absolute energy of –1327.17095670 hartree;
[h]absolute energy of –1327.15310268 hartree;
[i]absolute energy of –1327.22424170 hartree;
[j]absolute energy of –1327.17019415 hartree

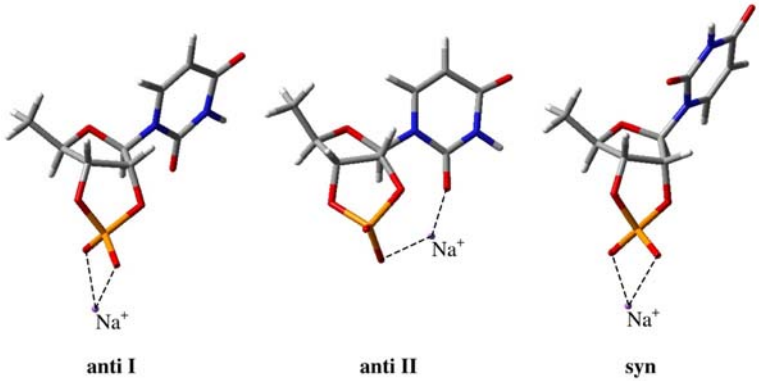

Fig. 6 Aqueous phase optimized structures of *anti* (**I** and **II**) and *syn* (right) DcUMP neutralized by Na^+ cation. The dashed lines point at the closest oxygen atoms (see text)

Table 4 Point charges derived from Mulliken (MPA), natural population analysis (NPA) and ChelpG (CHG) population analyses

	syn-DcUMP			*syn*-DcUMP Na^+		
	MPA	NPA	CHG	MPA	NPA	CHG
H5‴	0.128	0.202	0.045	0.139	0.210	0.067
H5″	0.118	0.199	0.071	0.134	0.210	0.091
H5′	0.128	0.200	0.080	0.146	0.212	0.094
C5′	−0.656	−0.582	−0.316	−0.521	−0.586	−0.315
C4′	0.120	0.092	0.372	0.337	0.105	0.306
H4′	0.146	0.210	0.017	0.129	0.194	0.022
O4′	−0.389	−0.619	−0.498	−0.383	−0.607	−0.469
C1′	0.108	0.294	0.186	−0.068	0.317	0.300
H1′	0.159	0.223	0.135	0.116	0.197	0.051
N1	0.176	−0.486	−0.211	0.134	−0.499	−0.335
C6	0.352	0.117	0.135	0.144	0.099	0.161
H6	0.123	0.220	0.111	0.111	0.214	0.118
C5	−0.114	−0.377	−0.503	−0.109	−0.354	−0.490
H5	0.093	0.228	0.166	0.109	0.238	0.178
C4	0.390	0.652	0.850	0.363	0.654	0.846
O4	−0.526	−0.640	−0.646	−0.483	−0.603	−0.598
N3	−0.520	−0.645	−0.707	−0.529	−0.638	−0.692
H3	0.267	0.414	0.354	0.283	0.422	0.366
C2	0.631	0.843	0.817	0.661	0.843	0.831
O2	−0.493	−0.634	−0.607	−0.495	−0.644	−0.617
C3′	0.135	0.099	0.397	−0.070	0.096	0.441
H3′	0.067	0.182	−0.037	0.133	0.222	0.007
C2′	−0.487	0.085	0.187	−0.298	0.096	0.301
H2′	0.106	0.205	0.035	0.130	0.212	−0.011
O2′	−0.498	−0.835	−0.587	−0.496	−0.840	−0.579
O3′	−0.491	−0.838	−0.613	−0.483	−0.830	−0.612
P	1.280	2.484	1.326	1.656	2.495	1.316
O1P	−0.590	−1.125	−0.746	−0.644	−1.197	−0.803
O2P	−0.763	−1.170	−0.814	−0.722	−1.205	−0.829
Na	–	–	–	0.576	0.967	0.853

formers). Therefore, for the purpose of the IPCM calculations, only two lowest energy forms of each conformer were chosen. The relative energy difference changed from 2.7 kcal mol^{-1} to 12 kcal mol^{-1} upon inclusion of aqueous environment. As in previous cases, the *syn*-conformer again proved to be more stable than *anti*-one.

As far as geometry changes are concerned, the most important structural features can be summarized as follows:

(i) *Syn*-conformation of the nucleobase: The most distinct structural feature of both derivatives, different from observed in other pyrimidine nucleotides, is the *syn*-conformation of their glycosidic bonds, which corresponds to a torsional angle $\chi \sim 65°$ (see Table 1)

(ii) Atypical sugar conformation: Another important conformational parameter is the pucker of the ribofuranose moiety. The phase angles of pseudorotation, *P*, are listed in the Table 1. Almost all values lie outside the preferred range of (ribo)nucleotides, i.e., $P = 340°–40°$ for the C3′-*endo* and $P = 140°–200°$ for the C2′-*endo*. The only exception is *anti*/*endo*-DcUMP, which preserved its original 3′-endo conformation. Sugar rings in the rest of cyclic nucleotides are considerably flattened compared with those of the normal nucleotide sugar rings. This is, most likely, a consequence of the rigidity imposed upon them by the cyclic ester linkage. Interestingly, the calculated maximum puckering amplitudes are not significantly different from the average value of 38.6 observed in standard sugars. [3] Only the *syn*/*exo*-conformer of DcUMP has a ν_{max} value lower than 30.

(iii) Conformational coupling in the bicyclic system: There is an evident connection between the puckering modes of sugar and phosphate moieties (see Table 1)—the *endo* form of cyclic phosphate exists with the ${}^0E$ form of the ribose, the *exo*-one with ${}_4E$. In the case of an *endo*-puckered phosphate ring, the O2P oxygen atom is involved in interactions with adjacent H(1′) and H(4′) atoms. The interatomic distances range from 2.33 Å to 2.79 Å and the P-O1P bond length is 0.02 Å longer than the corresponding bond length in *exo* conformer.

(iv) C-H···O intramolecular hydrogen bond: In case of *anti* 5′-O-methyl-cUMP, the distance between H(6) and O(5′) is 2.25 Å. This distance is less than the sum of oxygen and hydrogen van der Waals radii, so a potential hydrogen bond can be assumed. Additionally, a significant elongation (about 0.03 Å) of glycosidic bond in the *anti*-conformer is observed, supporting the suggestion of a possible HB existence. In case of 5′-deoxy-cUMP, the structure is devoid of the acceptor oxygen atom and thus the intramolecular H-bond cannot be created. It seems that, in this case, the major stabilizing

Table 5 Point charges derived from Mulliken (MPA), natural population analysis (NPA) and ChelpG (CHG) population analyses

	anti-DcUMP			*anti*-DcUMP Na^+		
	MPA	NPA	CHG	MPA	NPA	CHG
H5‴	0.136	0.209	0.056	0.143	0.214	0.072
H5″	0.123	0.202	0.075	0.142	0.215	0.102
H5′	0.107	0.187	0.057	0.128	0.200	0.080
C5′	−0.600	−0.580	−0.307	−0.559	−0.584	−0.297
C4′	0.191	0.083	0.373	0.242	0.095	0.241
H4′	0.169	0.224	0.034	0.140	0.201	0.059
O4′	−0.386	−0.627	−0.531	−0.345	−0.611	−0.443
C1′	−0.019	0.286	0.182	−0.341	0.290	0.100
H1′	0.219	0.251	0.153	0.205	0.241	0.154
N1	0.079	−0.490	−0.184	0.094	−0.501	−0.180
C6	0.210	0.105	0.163	0.178	0.089	0.147
H6	0.134	0.220	0.090	0.136	0.219	0.096
C5	−0.395	−0.373	−0.497	−0.302	−0.350	−0.478
H5	0.091	0.226	0.164	0.107	0.236	0.179
C4	0.384	0.652	0.821	0.380	0.654	0.822
O4	−0.532	−0.639	−0.640	−0.495	−0.605	−0.595
N3	−0.512	−0.647	−0.664	−0.513	−0.642	−0.683
H3	0.272	0.415	0.352	0.284	0.421	0.371
C2	0.751	0.839	0.745	0.763	0.840	0.761
O2	−0.468	−0.623	−0.591	−0.469	−0.629	−0.589
C3′	0.008	0.096	0.346	−0.128	0.096	0.362
H3′	0.062	0.173	−0.041	0.102	0.196	−0.013
C2′	−0.074	0.095	0.288	0.122	0.094	0.317
H2′	0.076	0.176	−0.047	0.111	0.199	−0.026
O2′	−0.498	−0.826	−0.566	−0.458	−0.821	−0.499
O3′	−0.483	−0.835	−0.601	−0.465	−0.826	−0.521
P	1.278	2.479	1.297	1.534	2.491	1.166
O1P	−0.581	−1.123	−0.738	−0.608	−1.186	−0.751
O2P	−0.740	−1.158	−0.792	−0.744	−1.208	−0.816
Na	–	–	–	0.616	0.968	0.863

contribution comes from interactions between the uracil O(2) atom and the H(3′) and H(2′) atoms of the sugar moiety.

Conclusions

In this paper, we have presented the results of DFT-based investigation on the conformational preferences of two uridine 2′,3′-cyclic monophosphate derivatives. The most remarkable structural feature revealed during this investigation is the unusual *syn*-orientation of the pyrimidine ring in the both cases analyzed. Although, for the isolated molecules, the energy differences between *syn*- and *anti*-conformers are small—less than 1 kcal mol^{-1}, they increase significantly up to 14 kcal mol^{-1} in aqueous solution. Moreover, for the minimum-energy gas-phase structures, the *endo*-type of puckering of the phosphate ring is observed, while in aqueous phase the *exo*-one is preferred. The rationale for such preferential hydration of the *syn*/*exo*-form stems most likely from their larger dipole moment and favorable exposure of phosphate oxygens, bearing high negative charges, capable of binding solvent molecules.

Acknowledgements The authors are grateful to the Polish State Committee for Scientific Research for financial support within grants: 4 T09A 185 25 (2003–2006) and 3 T09A 080 28 (2005–2006).

References

1. Haschmeyer AEV, Rich A, (1967) J Mol Biol. 27:369–384
2. Davies DB, (1978) Prog Nucl Magn Reson Spectrosc 12:135–225
3. Berthod H, Pullman B, (1971) Biochim Biophys Acta. 232:595–606
4. Hocquet N, Leulliot M, Ghomi M, (2000) J Phys Chem B 104:4560–4568
5. Jeffrey GA, Saenger W, (1991) Hydrogen Bonding in Biological Structures Springer Berlin
6. Saenger W, (1984) Principles of Nucleic Acid Structure Springer-Verlag New York
7. Desiraju GR, (1996) Acc Chem Res. 29:441–449
8. Castellano RK, (2004) Curr Org Chem. 8:845–865
9. Coulter CL, (1973) J Am Chem Soc. 95:570–575
10. Gelbin A, Schneider B, Clowney L, Hsieh S, Olson WK, Berman HM, (1996) J Am Chem Soc. 118:519–529
11. Hobza P, Sponer J, (1999) Chem Rev. 99:3247–3276
12. Foloppe N, MacKerell Jr AD, (1998) J Phys Chem B 102:6669–6678
13. Wlodawer A, Miller M, Sjölin L, (1983) Proc Natl Acad Sci. 80:3628–3631
14. Lavallee DK, Coulter CL, (1973) J Am Chem Soc. 95:576–581
15. Frisch MJ, Trucks G, Schlegel HB, Scuseria GE, Robb MA, Cheeseman JR, Montgomery JA Jr, Vreven T, Kudin KN, Burant JC, Millam JM, Iyengar SS, Tomasi J, Barone V, Mennucci B, Cossi M, Scalmani G, Rega N, Petersson GA, Nakatsuji H, Hada M, Ehara M, Toyota K, Fukuda R, Hasegawa J, Ishida M, Nakajima T, Honda Y, Kitao O, Nakai H, Klene M, Li X, Knox JE, Hratchian HP, Cross JB, Bakken V, Adamo C, Jaramillo J, Gomperts R, Stratmann RE, Yazyev O, Austin AJ, Cammi R, Pomelli C, Ochterski JW, Ayala PY, Morokuma K, Voth GA, Salvador P, Dannenberg JJ, Zakrzewski VG, Dapprich S, Daniels AD, Strain

MC, Farkas O, Malick DK, Rabuck AD, Raghavachari K, Foresman JB, Ortiz JV, Cui Q, Baboul AG, Clifford S, Cioslowski J, Stefanov BB, Liu G, Liashenko A, Piskorz P, Komaromi I, Martin RL, Fox DJ, Keith T, Al-Laham MA, Peng CY, Nanayakkara A, Challacombe M, Gill PMW, Johnson B, Chen W, Wong MW, Gonzalez C, Pople JA, (2003) Gaussian 03, Revision B.05 Gaussian Inc Pittsburgh PA
16. Becke AD, (1988) Phys Rev B 38:3098–3100
17. Lee C, Yang W, Parr RG, (1988) Phys Rev B 37:785–789
18. Hehre WJ, Ditchfield R, Pople JA, (1972) J Chem Phys. 56:2257–2261
19. Krishnan R, Binkley JS, Seeger R, Pople JA, (1980) J Chem Phys. 72:650–654
20. Hoffmann M, Rychlewski J, (2000) Computat Methods Sci Technolog. 6:61–64
21. Koch W, Holthausen MC, (2001) A Chemist's Guide to Density Functional Theory. Wiley-VCH, Weinheim
22. Mulliken RS, (1962) J Chem Phys. 36:3428–3439
23. Breneman CM, Wiberg KB, (1990) J Comp Chem. 11:361–373
24. Reed AE, Weinstock RB, Weinhold F, (1985) J Chem Phys. 83:735–746
25. Foresman JB, Keith TA, Wiberg KB, Snoonian J, Frisch MJ, (1996) J Phys Chem. 100:16098–16104
26. Altona C, Sundaralingam M, (1972) J Am Chem Soc. 94:8205–8212
27. Florian J, Baumruk V, Strajbl M, Bednarova L, Stepanek J, (1996) J Phys Chem. 100:1559–1568
28. Bachrach SM, (1994) Population Analysis and Electron Densities from Quantum Mechanics In: Lipkowitz KB, Boyd DB, (eds) Reviews in Computational Chemistry, Vol 5 VCH Publishers New York pp 171–227